Electronic Supplementary Material (ESI) for CrystEngComm.

Supplementary Information

Morphogenesis mechanisms in the hydrothermal growth of lead-free BCZT nanostructured multipods

Zouhair Hanani,[a,b,c] El-houssaine Ablouh,[d] Soukaina Merselmiz,[a] Jaafar Ghanbaja,[e] M'barek Amjoud,[a] Daoud Mezzane,[a,f] Abdelhadi Alimoussa,[a] Mohammed Lahcini,[a] Matjaž Spreitzer,[c] Damjan Vengust,[c] Mimoun El Marssi,[f] Igor A. Luk'yanchuk,[f,g,*] Zdravko Kutnjak,[c] and Mohamed Gouné[b]

[a] IMED-Lab, Cadi Ayyad University, Marrakesh, 40000, Morocco
[b] ICMCB, University of Bordeaux, Pessac, 33600, France
[c] Jozef Stefan Institute, Ljubljana, 1000, Slovenia
[d] MSN, Mohammed VI Polytechnic University, Ben Guerir, 43150, Morocco
[e] IJL, University of Lorraine, 54000, Nancy, France
[f] LPMC, University of Picardy Jules Verne, Amiens, 80039, France
[g] Department of Building Materials, Kyiv National University of Construction and Architecture, Kyiv, 03680, Ukraine

[*] Corresponding author: e-mail: lukyanc@ferroix.net

S1. Reagents and materials

Titanium isopropoxide ($Ti(OC_3H_7)_4$, ≥98.0%) was obtained from Merk, zirconium n-propoxide solution ($Zr(OCH_2CH_2CH_3)_4$, 70 wt. % in 1-propanol). Barium acetate ($Ba(CH_3COO)_2$, ACS reagent, 99.0-102.0%) was obtained from Alfa Aesar. Calcium nitrate tetrahydrate ($Ca(NO_3)_2{\cdot}4H_2O$, ACS reagent, 99%), ethanol (CH_3CH_2OH, laboratory reagent, 96%), isopropanol ($(CH_3)_2CHOH$, ACS reagent, ≥99.5%), sodium hydroxide pellets (NaOH, puriss. p.a. ACS reagent, ≥98%), hydrochloric acid (HCl, ACS reagent, 37%) were purchased from Sigma Aldrich. Potassium hydroxide pellets (KOH, ACS Reagent, ≥85%) was obtained from Honeywell Fluka. All reagents were used as received without further purification. Deionized water with resistivity of 18.2 MΩ cm^{-1} was obtained from a PURELAB-classic water purification system (ELGA LabWater), and was used for the experiments conducted in this work.

S2. Morphogenesis in *x*B*y*h powders

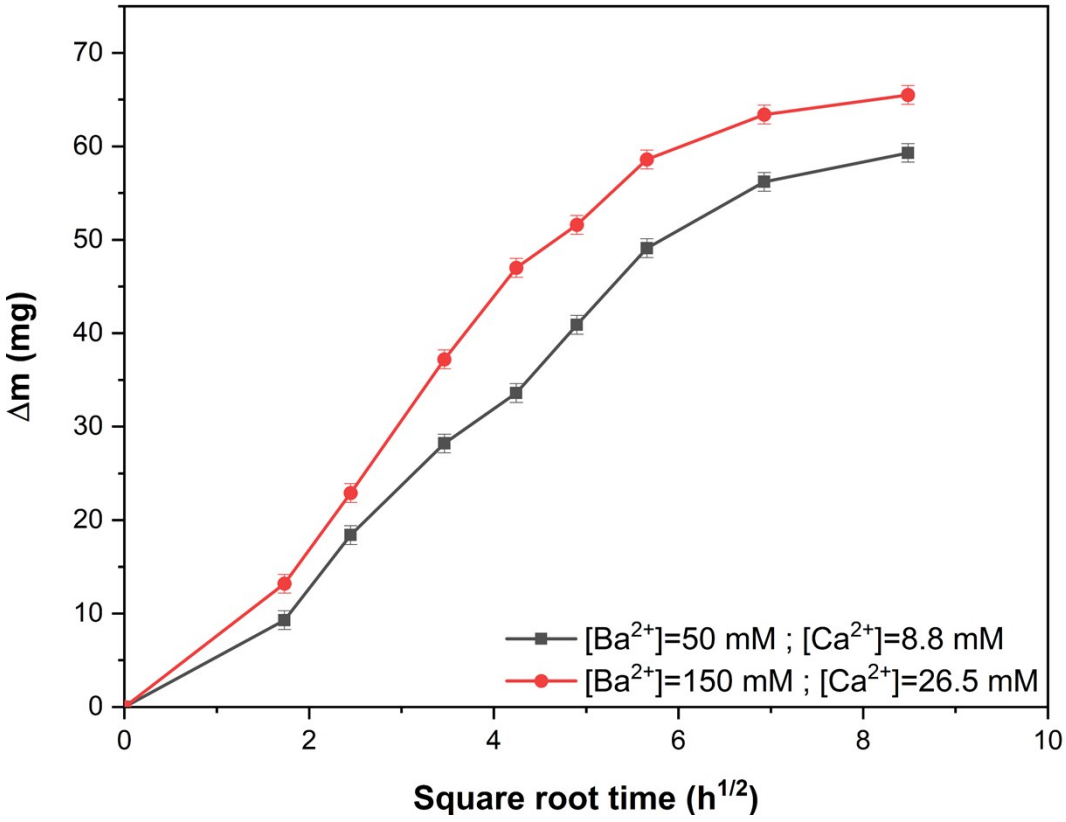

Fig. S1 Variation of samples' weight as a function of the reaction time.

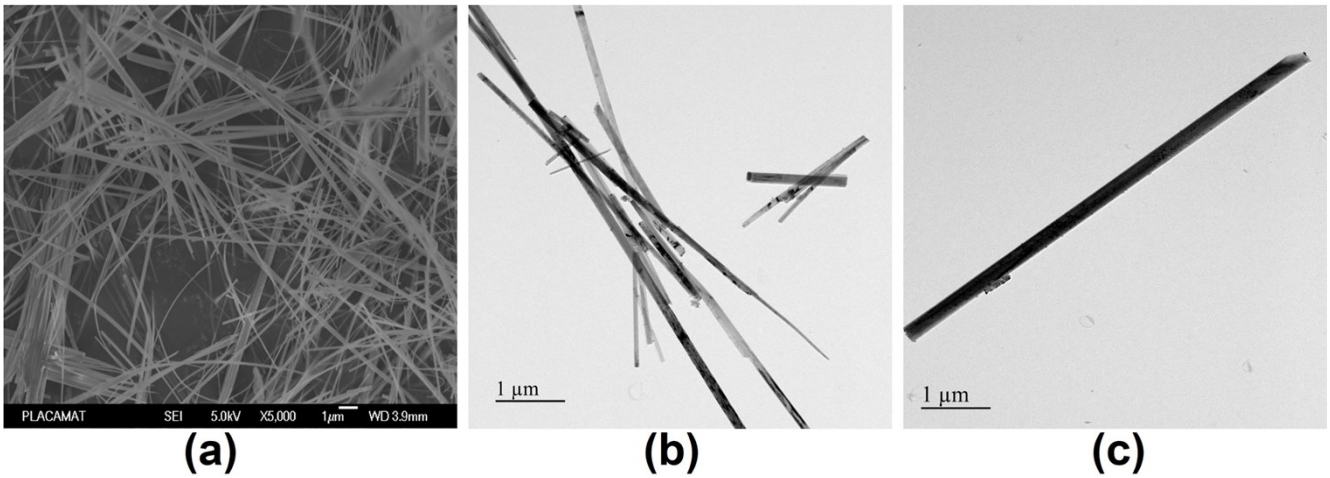

Fig. S2 (a) FESEM and TEM images of (b) HZTO-NWs and (c) a single HZTO-NW.

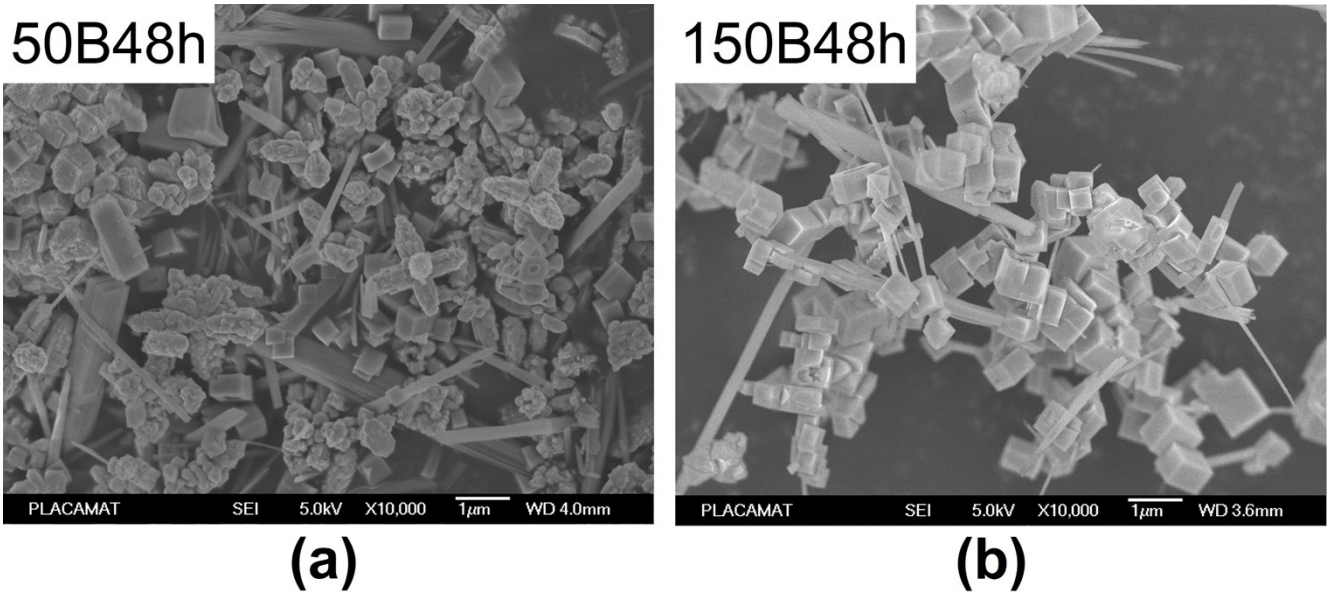

Fig. S3 FESEM images indicating the effect of A-site concentrations on the morphogenesis of BCZT materials after 48 h of hydrothermal reaction, using (a) 50 mM of Ba^{2+} and (b) 150 mM of Ba^{2+}.

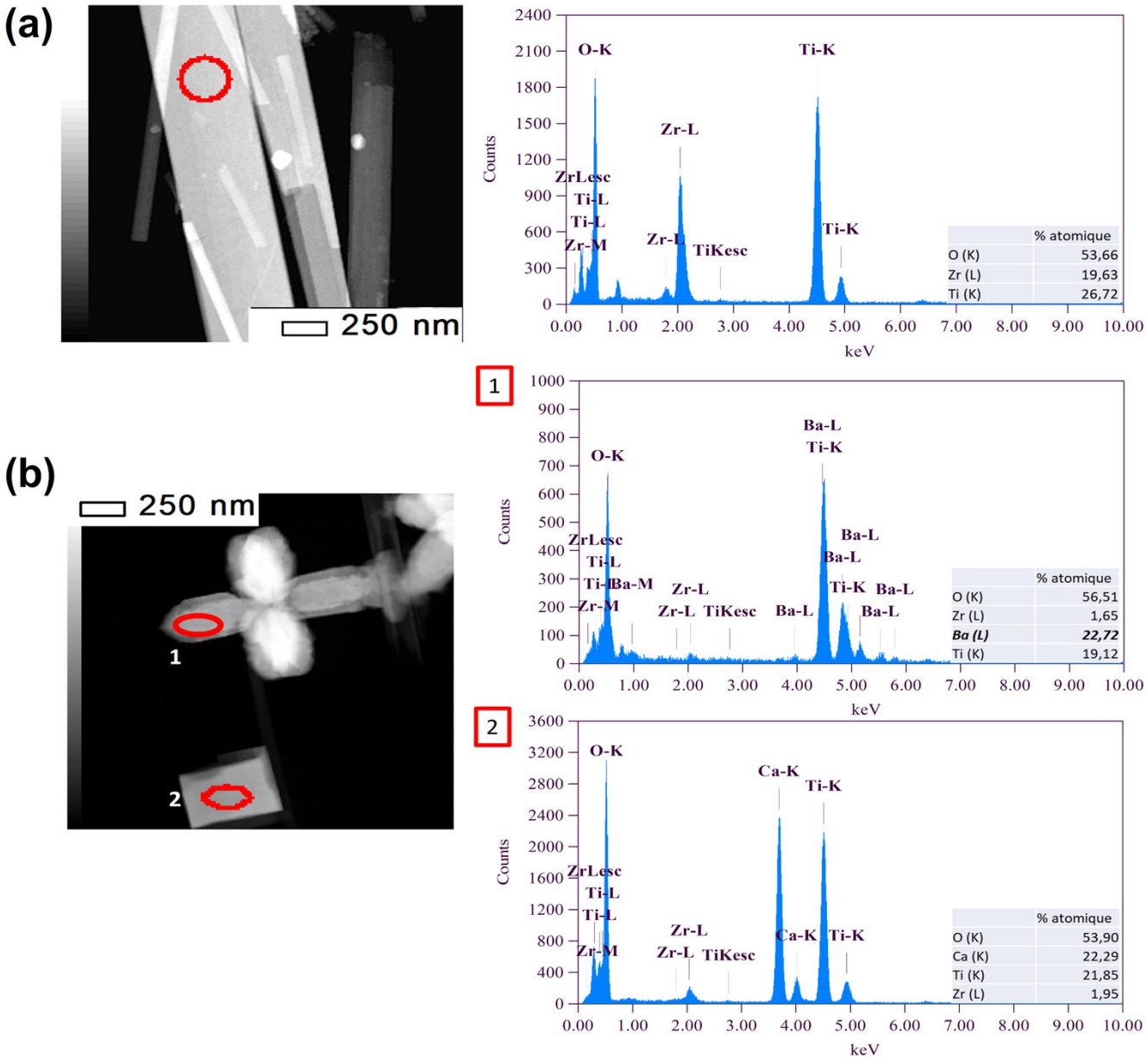

Fig. S4 TEM images and EDS spectra of (a) wire and (b) cube and multipod.

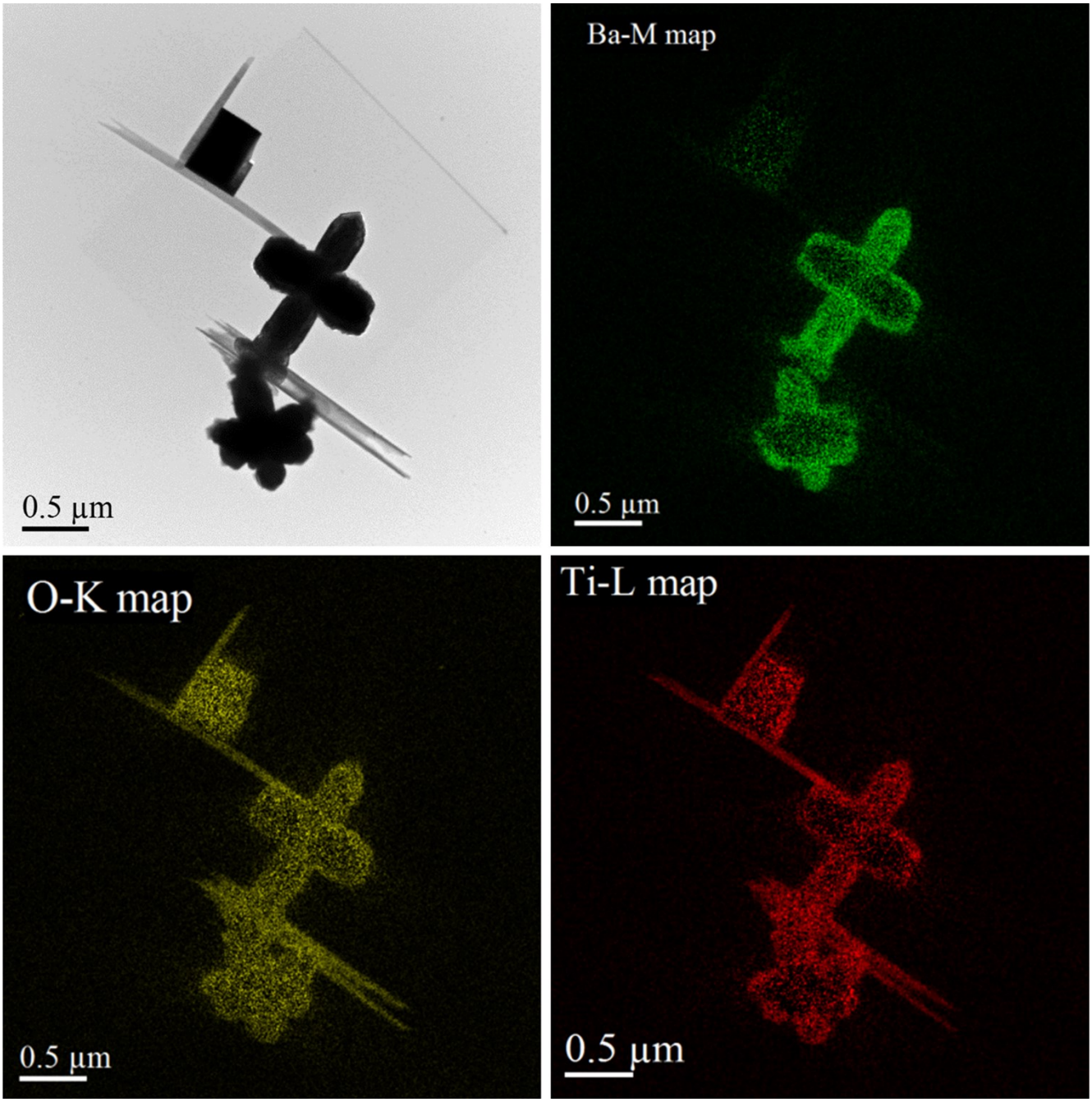

Fig. S5 EFTEM mapping images demonstrating the chemical composition of wire, cube and multipod.

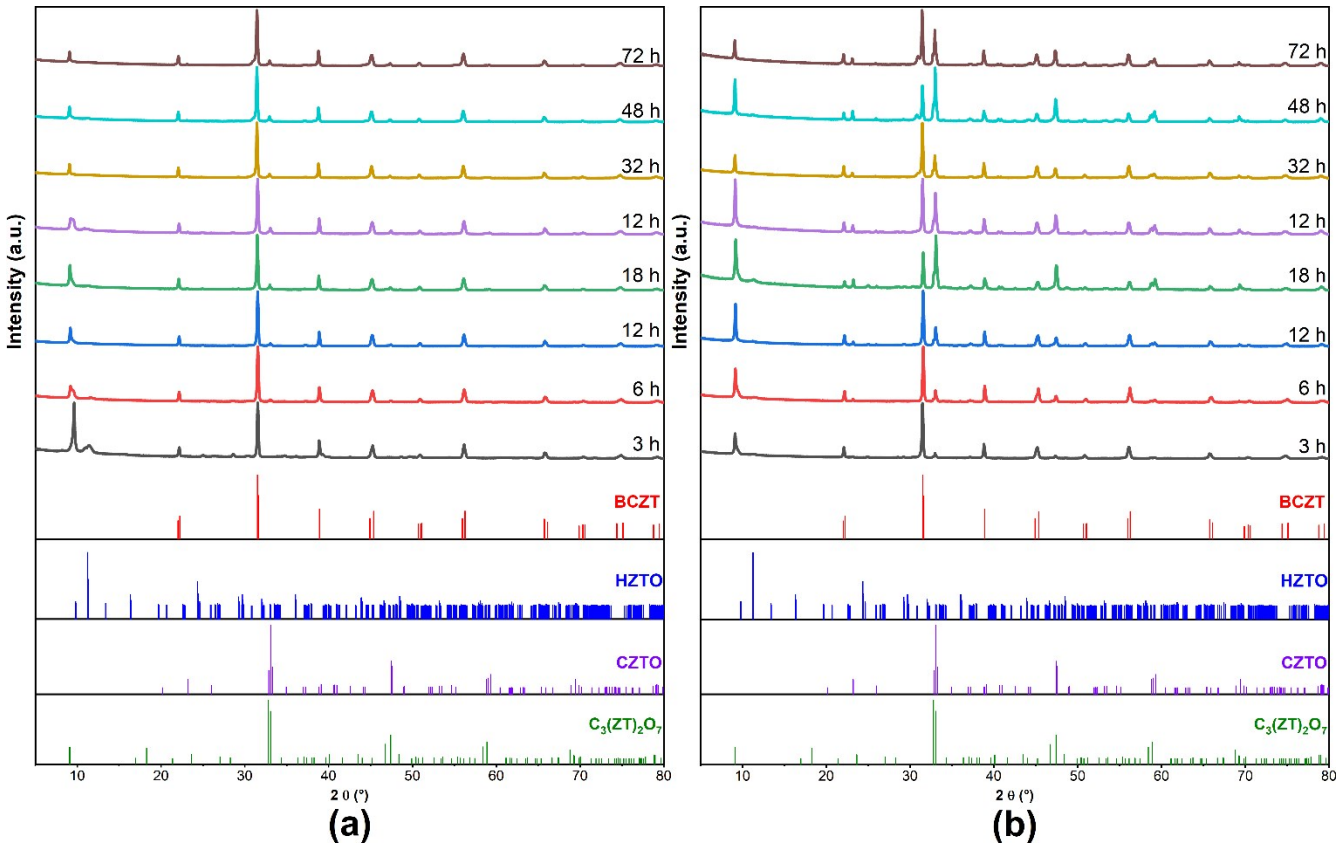

Fig. S6 XRD patterns of different *x*B*y*h powders elaborated using (a) {[Ba^{2+}] = 50 mM, [Ca^{2+}] = 8.8 mM} and (b) {[Ba^{2+}] = 150 mM, [Ca^{2+}] = 26.5 mM}, at various hydrothermal reaction times.

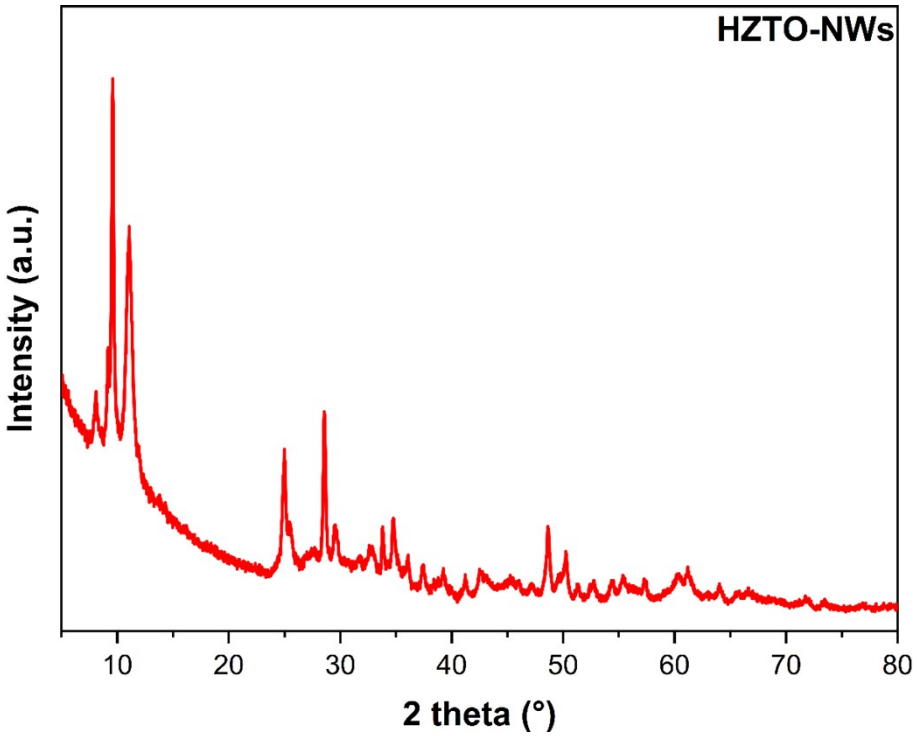

Fig. S7 XRD pattern of HZTO-NWs.

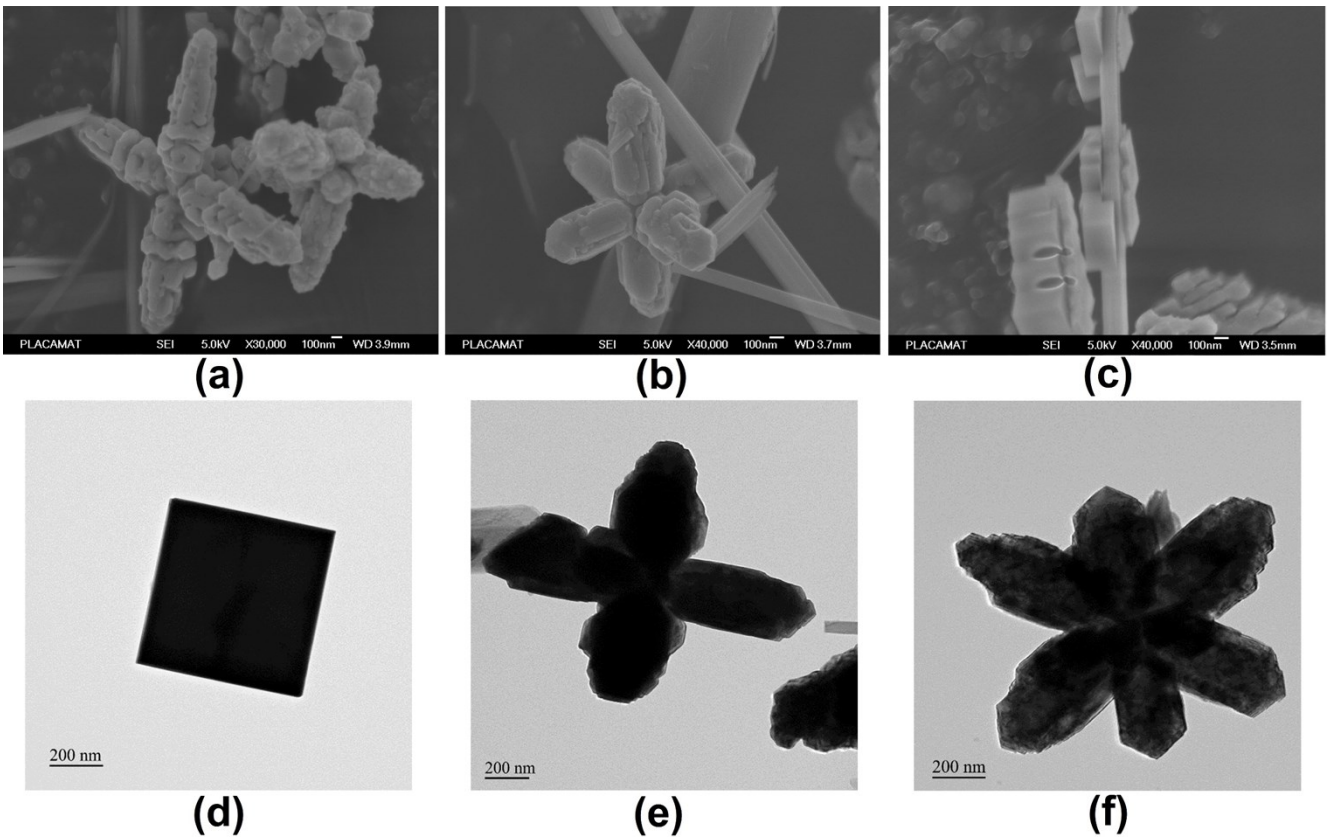

Fig. S8 (a-c) FESEM and (d-f) TEM images of various loose nanostructures using 150 mM of Ba^{2+} and 26.5 mM of Ca^{2+}.

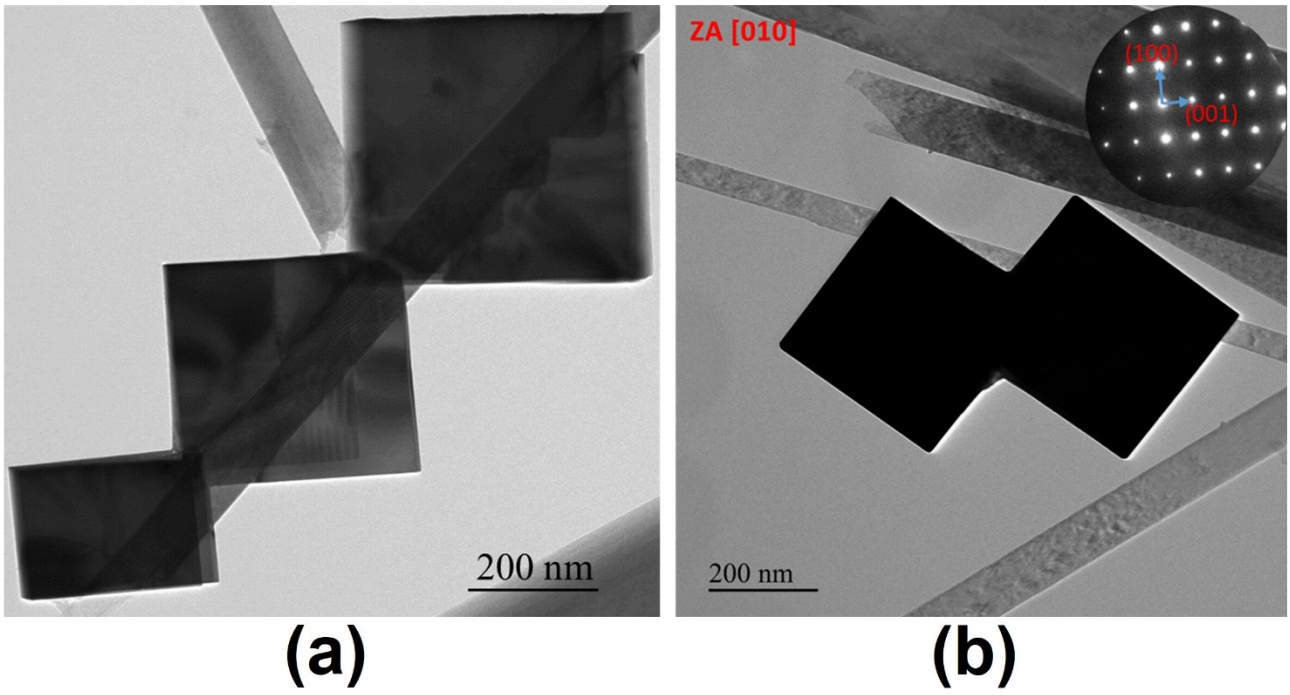

Fig. S9 TEM images of (a) three edge-attached cubes and (b) two edge-attached cubes (SAED pattern in inset).